arXiv:1609.08365v1 [math.CA] 27 Sep 2016

# Asymptotics of a Gauss hypergeometric function with large parameters, III: Application to the Legendre functions of large imaginary order and real degree

R. B. Paris*

*Division of Computing and Mathematics,*
*University of Abertay Dundee, Dundee DD1 1HG, UK*

**Abstract**

We obtain the asymptotic expansion for the Gauss hypergeometric function

$$F(a-\lambda, b+\lambda; c+i\alpha\lambda; z)$$

for $\lambda \to +\infty$ with $a$, $b$ and $c$ finite parameters by application of the method of steepest descents. The quantity $\alpha$ is real, so that the denominatorial parameter is complex and $z$ is a finite complex variable restricted to lie in the sector $|\arg(1-z)| < \pi$. We concentrate on the particular case $a = 0$, $b = c = 1$, which is associated with the Legendre functions of real degree and imaginary order. The resulting expansions are of Poincaré type and hold in restricted domains of the $z$-plane. An expansion is given at the coalescence of two saddle points. Numerical results illustrating the accuracy of the different expansions are given.

**MSC:** 33C05, 34E05, 41A60

**Keywords:** Hypergeometric function, asymptotic expansion, large parameters, steepest descents, Legendre functions

## 1. Introduction

The Gauss hypergeometric function is defined by

$$F\left(\begin{matrix}a, b\\ c\end{matrix}; z\right) = \sum_{n=0}^{\infty} \frac{(a)_n (b)_n}{(c)_n n!}\, z^n \qquad (|z| < 1)$$

and elsewhere by analytic continuation, where $(a)_n = \Gamma(a+n)/\Gamma(a) = a(a+1)\ldots(a+n-1)$ is the Pochhammer symbol or rising factorial. The asymptotic expansion of

$$F\left(\begin{matrix}a+\epsilon_1\lambda, b+\epsilon_2\lambda\\ c+\epsilon_3\lambda\end{matrix}; z\right)$$

for large values of $\lambda$ and fixed complex $z$ when the parameters $\epsilon_j$ are finite was first considered by Watson [16] in 1918 and recently by the author in [13, 14]; see also [4] for the case of two large parameters. This function may be characterised by the set $\{\epsilon_1, \epsilon_2, \epsilon_3\}$, where, by a rescaling of $\lambda$ one of the $\epsilon_j$ can (if so desired) always be replaced by unity. Watson considered the situation when $\epsilon_j = 0, \pm 1$ and examined the cases $(0, 0, 1)$, $(1, -1, 0)$ and $(0, -1, 1)$, together with the additional

*E-mail address: r.paris@abertay.ac.uk

case $(1,2,0)$. In [13, 14], the $\epsilon_j$ were taken to be positive constants. It was shown that it is sufficient to consider just three basic types of hypergeometric function corresponding to the parameter sets $(\epsilon,0,1)$ (Type A), $(\epsilon,-1,0)$ (Type B) and $(\epsilon_1,\epsilon_2,1)$ (Type C), where $\epsilon,\epsilon_1,\epsilon_2>0$. An application of the expansion for the case $(\epsilon,\epsilon,1)$ with $\epsilon>0$ has arisen in aerodynamics [3, 8]. Expansions of a uniform character when two parameters are large have been given for the case $(1,-1,0)$ in [7] and $(0,-1,1)$, $(1,2,0)$ in [9].

In this paper, we consider the expansion of the function

$$F\left(\begin{array}{c} a-\lambda, b+\lambda \\ c+i\alpha\lambda \end{array}; z\right) \tag{1.1}$$

for $\lambda\to+\infty$ with finite $a$, $b$ and $c$. Here the parameter $\alpha\in\mathbf{R}$ is finite and $z$ is a (finite) complex variable restricted to lie in $|\arg(1-z)|<\pi$. The parameter set in this case is consequently $(-1,1,i\alpha)$, which is different from the cases previously considered in that the denominatorial parameter $\epsilon_3=i\alpha$ is *purely imaginary*. As in [13, 14], we employ the method of steepest descents applied to a contour integral representation of the function in (1.1) to obtain Poincaré-type expansions. The expansion in the case of the coalescence of two saddle points is also considered.

We concentrate on the situation when the parameters in (1.1) have the values $a=0$, $b=c=1$ and consider the function

$$F_\alpha(\lambda;z):=F\left(\begin{array}{c} -\lambda, 1+\lambda \\ 1+i\alpha\lambda \end{array}; z\right) \tag{1.2}$$

with $\alpha>0$. This particular case has arisen in the study of travelling waves in a Toda lattice [19, 17]. This case is also of interest as it is associated with the Legendre functions through the relations [11, p. 353]

$$P_\nu^{-\mu}(x)=\frac{1}{\Gamma(1+\mu)}\left(\frac{x-1}{x+1}\right)^{\mu/2}F(-\nu,1+\nu;1+\mu;\tfrac12-\tfrac12x) \tag{1.3}$$

and

$$\begin{aligned} e^{\pi i\mu}Q_\nu^{-\mu}(x)=&\frac{\Gamma(1+\nu-\mu)\Gamma(\mu)}{2\Gamma(1+\nu+\mu)}\left(\frac{x-1}{x+1}\right)^{-\mu/2}F(-\nu,1+\nu;1-\mu;\tfrac12-\tfrac12x)\\ &+\frac{\Gamma(-\mu)}{2}\left(\frac{x-1}{x+1}\right)^{\mu/2}F(-\nu,1+\nu;1+\mu;\tfrac12-\tfrac12x), \end{aligned} \tag{1.4}$$

which define the functions in the complex $x$-plane cut along $(-\infty,1]$. Thus, as a by-product of our investigation of (1.2) we will obtain the expansions of the Legendre functions $P_\lambda^{\pm i\alpha\lambda}(x)$ and $Q_\lambda^{\pm i\alpha\lambda}(x)$, for large imaginary order and real degree. The expansions for these functions when $x=\sqrt{1+\alpha^2}$, which corresponds to the above-mentioned coalescence of two saddle points, is also given. We remark that the expansion of $P_\nu^{-i\mu}(x)$ and $Q_\nu^{-i\mu}(x)$ for $\nu\to+\infty$, $\Re(x)\geq0$ uniformly valid for $0\leq\mu/(\nu+\frac12)\leq A$, where $A$ is a constant, has been considered by Dunster [6] who employed a differential-equation approach.

We remark that when $z=\frac12$ it is possible to give an exact evaluation for $F_\alpha(\lambda;z)$ in the form [11, (15.4.30)]

$$F_\alpha(\lambda;\tfrac12)=\frac{2^{-i\alpha\lambda}\sqrt{\pi}\,\Gamma(1+i\alpha\lambda)}{\Gamma(\frac12+\frac12\lambda(i\alpha-1))\Gamma(1+\frac12\lambda(i\alpha+1))}\ . \tag{1.5}$$

## 2. The expansion of $F_\alpha(\lambda;z)$ for $\lambda\to+\infty$

We take the parameter values $a=0$, $b=c=1$ in (1.1) and consider in detail the expansion of $F_\alpha(\lambda;z)$ in (1.2) for $\lambda\to+\infty$; the case of general values of $a$, $b$ and $c$ is considered in Section 2.3. From the series representation of the hypergeometric function it follows that, when $\lambda>0$ and $\alpha$ is real,

$$F_{-\alpha}(\lambda;z)=\overline{F}_\alpha(\lambda;\overline{z}), \tag{2.1}$$

where the bar denotes the complex conjugate. It is therefore sufficient to consider $\alpha > 0$ throughout; in addition, we define

$$\theta := \arg\, z, \qquad \phi := \arctan\, \alpha, \tag{2.2}$$

where $\theta \in [-\pi, \pi]$ and $\phi \in (0, \frac{1}{2}\pi)$.

We employ the integral representation [11, p. 388]

$$F\left(\begin{matrix} a, b \\ c \end{matrix}; z\right) = \frac{\Gamma(c)\Gamma(1+b-c)}{2\pi i \Gamma(b)} \int_0^{(1+)} \frac{t^{b-1}(t-1)^{c-b-1}}{(1-zt)^a}\, dt, \qquad \Re(b) > 0, \tag{2.3}$$

where it is supposed that $|\arg(1-z)| < \pi$ and $c - b \neq 1, 2, \ldots$ . The integration path is a closed loop that starts from the origin, encircles the point $t = 1$ in the positive sense and returns to the origin without enclosing the point $t = 1/z$. The function $F_\alpha(\lambda; z)$ can then be expressed in the form

$$F_\alpha(\lambda; z) = F\left(\begin{matrix} -\lambda, 1+\lambda \\ 1 + i\alpha\lambda \end{matrix}; z\right) = \frac{G_\alpha(\lambda)}{2\pi i} \int_0^{(1+)} f(t) e^{\lambda\psi(t)} dt, \tag{2.4}$$

where the phase function $\psi(t)$ and the amplitude function $f(t)$ are

$$\psi(t) = \log\, t(1-zt) - \beta \log(t-1), \qquad f(t) = (t-1)^{-1}, \qquad \beta := 1 - i\alpha \tag{2.5}$$

and

$$G_\alpha(\lambda) := \frac{\Gamma(1+i\alpha\lambda)\Gamma(1+\lambda\beta)}{\Gamma(1+\lambda)} = i\alpha\beta\lambda \frac{\Gamma(i\alpha\lambda)\Gamma(\lambda\beta)}{\Gamma(\lambda)}\ . \tag{2.6}$$

The $t$-plane is cut along $(-\infty, 1]$ and also along the ray from the singularity at $t = 1/z$ to infinity in a suitable direction.

The phase function has saddle points where $\psi'(t) = 0$; that is at the points where

$$\frac{i\alpha t_s - 1}{t_s(t_s - 1)} - \frac{z}{1 - zt_s} = 0.$$

There are consequently two saddle points, which we label $t_{s1}$ and $t_{s2}$, given by

$$t_{s1}, t_{s2} = \frac{z + \frac{1}{2}i\alpha \mp i(z - z^2 + \frac{1}{4}\alpha^2)^{1/2}}{(1+i\alpha)z}, \tag{2.7}$$

respectively. For sufficiently large $\lambda$, the points $t = 0$ and $t = 1/z$ are zeros of the integrand, so that paths of steepest descent can terminate only at these two points; paths of steepest ascent must terminate at $t = 1$ and at infinity. A typical arrangement of the steepest paths through $t_{s1}$ and $t_{s2}$ is shown in Fig. 1 when $\alpha = 1$ and for different values of $\theta$.

Since $t_{s1}t_{s2} = \{(1+i\alpha)z\}^{-1}$, it follows that

$$\arg\, t_{s1} + \arg\, t_{s2} = -(\theta + \phi).$$

Consequently, when $\theta + \phi > 0$ (resp. $< 0$) at *least* one saddle is situated in the lower (resp. upper) half-plane; when $\theta + \phi = 0$, one saddle is situated in upper half-plane with the other in the lower half-plane. It is to be noted that the saddles coalesce to form a double saddle when $z^2 - z - \frac{1}{4}\alpha^2 = 0$; that is when

$$z = z_d^{\pm} := \tfrac{1}{2} \pm \tfrac{1}{2}\sqrt{1+\alpha^2}. \tag{2.8}$$

The contribution to the integral (2.4) (excluding the pre-factor) from the steepest descent path through the (simple) saddle $t_{sj}$ is given by the formal asymptotic sum [1, p. 265]

$$if(t_{sj}) e^{\lambda\psi(t_{sj}) + \pi i\gamma_j} \sqrt{\frac{2\pi}{\psi''(t_{sj})}} \sum_{s=0}^{\infty} \frac{c_s^{(j)} (\frac{1}{2})_s}{\lambda^{s+\frac{1}{2}}} \qquad (j = 1, 2) \tag{2.9}$$

as $\lambda \to +\infty$, where

$$\psi''(t_{sj}) = -\frac{2}{(t_{sj}-1)^2}\left\{\left(1 - \frac{1}{t_{sj}}\right)\left(1 - \frac{1}{t_{sj}} - \beta\right) - \frac{1}{2}\beta(1-\beta)\right\}.$$

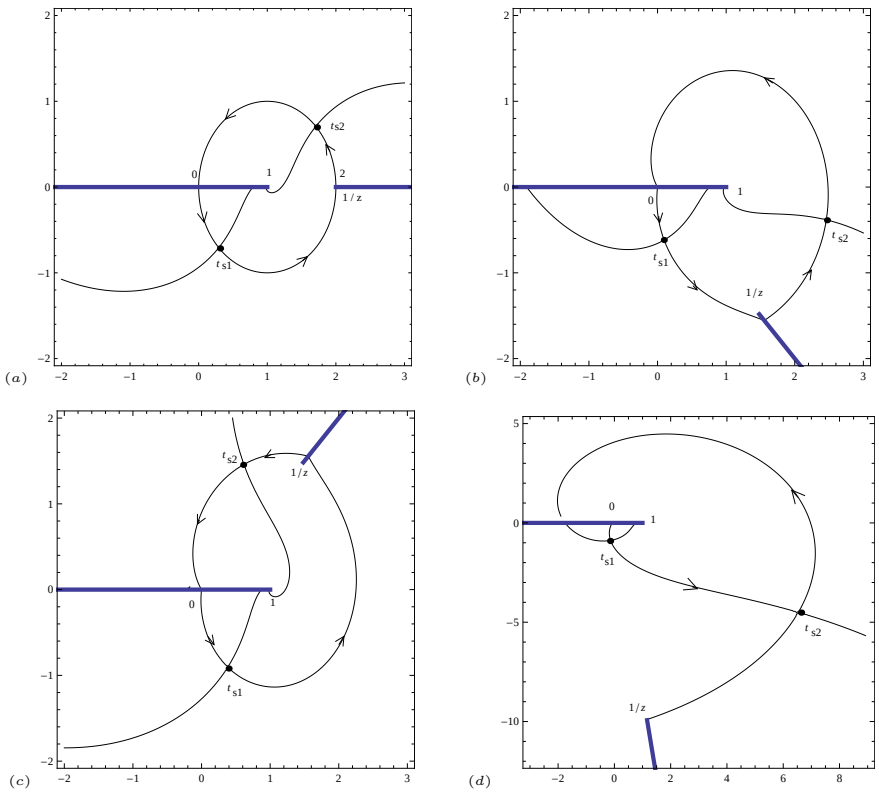


Figure 1: Examples of the steepest descent and ascent paths for $|z| = 0.50$ and $\alpha = 1$ when (a) $\theta = 0$, (b) $\theta = \frac{1}{4}\pi$ and (c) $\theta = -\frac{1}{4}\pi$; (d) $|z| = 0.10$, $\theta \doteq 0.46292\pi$ corresponding to a Stokes phenomenon. The saddles are denoted by heavy dots and the arrows indicate the integration path. There is a branch cut along $(-\infty, 1]$ and from the point $1/z$ out to infinity.

The $\gamma_j$ are orientation factors that depend on the direction of integration $\arg(t - t_{sj})$ through the saddle point $t_{sj}$ and have the value either 0 or 1.

**2.1 The coefficients $c_s^{(j)}$.** The coefficients $c_s^{(j)} \equiv c_s$ (which are functions of $\alpha$ and $z$) for $s \le 2$ are given explicitly by

$$c_0 = 1, \qquad c_1 = \frac{1}{2\psi''}\{2F_2 - 2\Psi_3 F_1 + \tfrac{5}{6}\Psi_3^2 - \tfrac{1}{2}\Psi_4\},$$

$$c_2 = \frac{1}{(2\psi'')^2}\{\tfrac{2}{3}F_4 - \tfrac{20}{9}\Psi_3 F_3 + \tfrac{5}{3}(\tfrac{7}{3}\Psi_3^2 - \Psi_4)F_2 - \tfrac{35}{9}(\Psi_3^3 - \Psi_3\Psi_4 + \tfrac{6}{35}\Psi_5)F_1$$
$$+\tfrac{35}{9}(\tfrac{11}{24}\Psi_3^4 - \tfrac{3}{4}(\Psi_3^2 - \tfrac{1}{6}\Psi_4)\Psi_4 + \tfrac{1}{5}\Psi_3\Psi_5 - \tfrac{1}{35}\Psi_6)\}, \tag{2.10}$$

where, for brevity, we have defined

$$\Psi_m := \frac{\psi^{(m)}(t)}{\psi''(t)} \quad (m \ge 3), \qquad F_m := \frac{f^{(m)}(t)}{f(t)} \quad (m \ge 1)$$

with $\psi(t)$, $f(t)$ and their derivatives being evaluated at $t = t_{s1}$ or $t = t_{s2}$; see, for example, [5, p. 119], [10, p. 127], [12, p. 13].

Alternatively, the $c_s$ can be obtained by an expansion process to yield Wojdylo's formula [18] given by

$$c_s = \frac{(-)^s}{\hat{\alpha}_0^s}\sum_{k=0}^{2s}\frac{\hat{\beta}_{2s-k}}{\hat{\beta}_0}\sum_{j=0}^{k}\frac{(-)^j(s+\frac{1}{2})_j}{j!\,\hat{\alpha}_0^j}\,\mathcal{B}_{kj}\,; \tag{2.11}$$

see also [15, p. 25]. Here $\mathcal{B}_{kj} \equiv \mathcal{B}_{kj}(\hat{\alpha}_1, \hat{\alpha}_2, \ldots, \hat{\alpha}_{k-j+1})$ are the partial ordinary Bell polynomials generated by the recursion[1]

$$\mathcal{B}_{kj} = \sum_{r=1}^{k-j+1} \hat{\alpha}_r \mathcal{B}_{k-r,j-1}, \qquad \mathcal{B}_{k0} = \delta_{k0},$$

where $\delta_{mn}$ is the Kronecker symbol, and the coefficients $\hat{\alpha}_r$ and $\hat{\beta}_r$ appear in the expansions

$$\psi(t) - \psi(t_s) = \sum_{r=0}^{\infty} \hat{\alpha}_r (t - t_s)^{r+2}, \qquad f(t) = \sum_{r=0}^{\infty} \hat{\beta}_r (t - t_s)^r$$

valid in a neighbourhood of the saddle $t = t_s$.

**2.2 The expansion of $F_\alpha(\lambda; z)$.** It can be seen from Fig. 1 that the *steepest ascent* path through $t_{s1}$ crosses the branch cut to pass onto an adjacent Riemann sheet in the $t$-plane. When $\theta$ increases, it is found that in some cases the saddle $t_{s2}$ (and consequently a portion of the associated steepest descent path) can also pass onto an adjacent sheet. To avoid this difficulty, we make the substitution $t = e^w$ to find the phase function in (2.5) given by

$$\psi(w) = (1 - \tfrac{1}{2}\beta)w + \log(1 - ze^w) - \beta \log\, 2\sinh \tfrac{1}{2}w,$$

with the image of the saddles given by $w_j = \log t_{sj}$ $(j = 1, 2)$. The closed circuit surrounding the point $t = 1$ in the $t$-plane becomes the loop that commences at $-\infty$, encircles the point $w = 0$ in the positive sense and returns to $-\infty$. Branch cuts are introduced along $(-\infty, 1]$ and from the point $\log 1/z$ out to $\infty$ parallel to the real $w$-axis. This transformation causes all the Riemann sheets in the $t$-plane to appear as horizontal strips of width $2\pi$ in the $w$-plane; the principal sheet corresponds to $-\pi < \Im(w) \leq \pi$.

Examples of the steepest paths in the $w$-plane are illustrated in Fig. 2. In Fig. 2(a) both the saddles $w_1$ and $w_2$ and their associated steepest descent paths are situated on the principal sheet; in Fig. 2(b) the saddles are again on the principal sheet, but the steepest descent path from $w_2$ crosses the line $\Im(w) = \pi$, which corresponds to passing on to the adjacent sheet in the $t$-plane. Fig. 2(c) shows the same situation as Fig. 1(d), namely $|z| = 0.10$, $\theta \doteq 0.46292\pi$; for this value of $\theta$ the saddles $w_1$ and $w_2$ are connected, with the steepest descent path from $w_2$ passing into the strip $\pi < \Im(w) \leq 3\pi$. The saddle in this strip corresponds to the image of the saddle $w_1$ in the principal sheet; the contribution from this image saddle is exponentially smaller (by the factor $e^{-2\pi\alpha\lambda}$) than that from $w_1$ and so is neglected. Fig. 2(d) shows $|z| = 0.10$, $\theta = 0.60\pi$ where the steepest descent path through $w_1$ has disconnected from the saddle $w_2$ (a Stokes phenomenon) and passes over into the adjacent strip.

Then, from (2.4), we have the expansion

$$F_\alpha(\lambda; z) \sim G_\alpha(\lambda) \left\{ \frac{e^{\lambda\psi(t_{s1})} f(t_{s1})}{\sqrt{2\pi\psi''(t_{s1})}} \sum_{s=0}^{\infty} \frac{c_s^{(1)} (\frac{1}{2})_s}{\lambda^{s+\frac{1}{2}}} + \frac{e^{\lambda\psi(t_{s2})} f(t_{s2})}{\sqrt{2\pi\psi''(t_{s2})}} \sum_{s=0}^{\infty} \frac{c_s^{(2)} (\frac{1}{2})_s}{\lambda^{s+\frac{1}{2}}} \right\} \tag{2.12}$$

as $\lambda \to +\infty$ valid for complex $z$ in $|\arg(1 - z)| < \pi$. This expansion will break down in the neighbourhood of the double saddle points at $z = z_d^{\pm}$, and also ceases to be valid in a zone surrounding $z = 0$; see below. The orientation factors $\gamma_1 = \gamma_2 = 0$ and we note that

$$e^{\lambda\psi(t_{sj})} = \left\{ \frac{t_{sj}(1 - zt_{sj})}{(t_{sj} - 1)^\beta} \right\}^\lambda.$$

If required, an expansion for $G_\alpha(\lambda)$ in inverse powers of $\lambda$ is given in the appendix.

The boundary in the upper-half $z$-plane on which $\Re\psi(t_{s1}) = \Re\psi(t_{s2})$ is shown in Fig. 3 for the particular case of $\alpha = 1$. This curve has its endpoints $A$ and $B$ at the double saddle points $z_d^{\pm}$ in (2.8). Below this curve, and also in $\Im(z) < 0$, the contribution from the saddle $t_{s1}$ dominates that from the saddle $t_{s2}$; above this curve the saddle $t_{s2}$ is dominant. In the neighbourhood of the curve both contributions need to be taken into account.

[1] For example, this generates the values $\mathcal{B}_{41} = \hat{\alpha}_4$, $\mathcal{B}_{42} = \hat{\alpha}_2^2 + 2\hat{\alpha}_1\hat{\alpha}_3$, $\mathcal{B}_{43} = 3\hat{\alpha}_1^2\hat{\alpha}_2$ and $\mathcal{B}_{44} = \hat{\alpha}_1^4$.

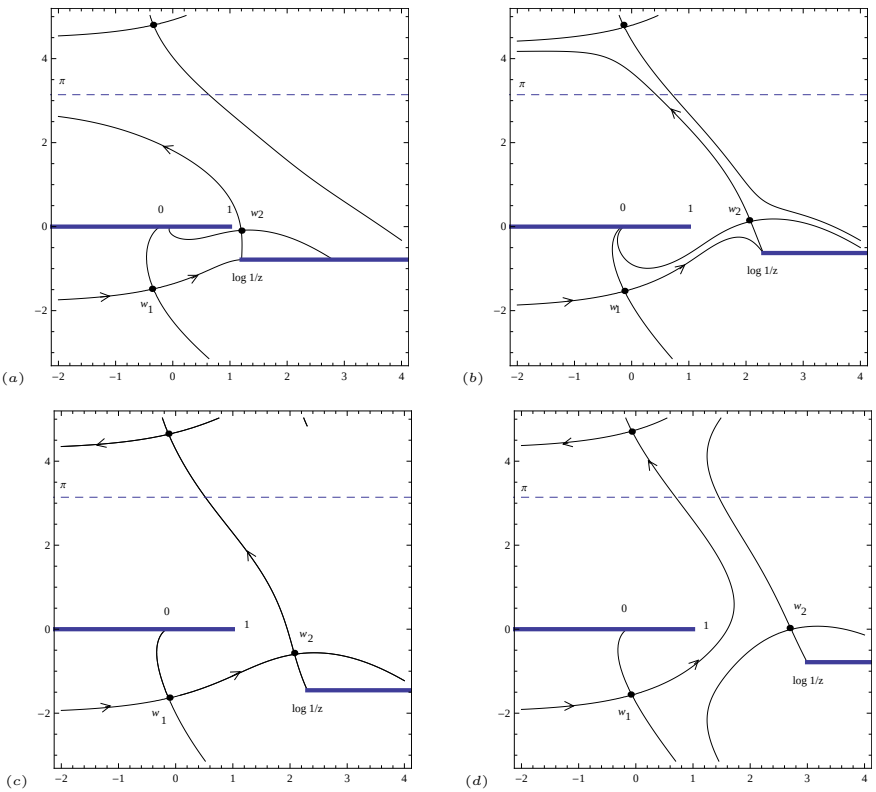


Figure 2: Examples of the steepest descent and ascent paths in the $w$-plane for $\alpha = 1$ when (a) $|z| = 0.30$, $\theta = 0.25\pi$, (b) $|z| = 0.10$, $\theta = 0.20\pi$, (c) $|z| = 0.10$, $\theta \doteq 0.46292\pi$ corresponding to a Stokes phenomenon and (d) $|z| = 0.10$, $\theta = 0.60\pi$. The saddles are denoted by heavy dots and the arrows indicate the integration path. There is a branch cut along $(-\infty, 1]$ and from the point $\log 1/z$ out to infinity.

The dashed closed curve surrounding $z = 0$ (the enclosed domain is denoted by $\mathcal{D}$) and terminating at $z_d^-$ shows the curve on which $\Im\psi(t_{s1}) = \Im\psi(t_{s2})$, where a Stokes phenomenon occurs. As one crosses this loop and passes into its interior the saddle $t_{s2}$ disconnects from the integration path to leave only the contribution from the saddle $t_{s1}$; see Fig. 1(d) and Fig. 2(c), (d). As a consequence, the expansion of $F_\alpha(\lambda; z)$ inside this loop is given by

$$F_\alpha(\lambda; z) \sim G_\alpha(\lambda) \frac{e^{\lambda\psi(t_{s1})} f(t_{s1})}{\sqrt{2\pi\psi''(t_{s1})}} \sum_{s=0}^{\infty} \frac{c_s^{(1)} (\frac{1}{2})_s}{\lambda^{s+\frac{1}{2}}} \qquad (z \in \mathcal{D}) \tag{2.13}$$

as $\lambda \to +\infty$.

In the lower-half $z$-plane, the saddle $t_{s2}$ can pass over onto an adjacent Riemann sheet (in the $t$-plane) and great care must be taken to ensure that one uses continuous branches for the functions $\log t_{s2}$ and $\log(t_{s2} - 1)$. The curves on which $t_{s2}$ and $t_{s2} - 1$ pass onto adjacent sheets are indicated in Fig. 3 by the dotted curves issuing from $z = 0$ and $z = 1$, respectively. To the right (resp. left) of the curve issuing from $z = 0$ (resp. $z = 1$), $t_{s2}$ (resp. $t_{s2} - 1$) lies on the principal sheet. It must be emphasised that all the curves in Fig. 3 depend on the value of the parameter $\alpha > 0$.

The results of numerical computations carried out with *Mathematica* are presented in Tables 1 and 2. Table 1 shows the absolute relative error[2] in the computation of $F_\alpha(\lambda; z)$ as a function of the truncation index $s$ for $\alpha = 1$, $\lambda = 80$ and $z = 0.50e^{i\theta}$ using the expansion (2.12). We note that when $\theta = 0$ the value of $F_\alpha(\lambda; \frac{1}{2})$ is given by (1.5). The coefficients $c_s^{(1,2)}$ were derived from (2.11) and the high-precision evaluation of $F_\alpha(\lambda; z)$ obtained by the routine Hypergeometric2F1 in *Mathematica*. Table 2 shows the absolute relative error as a function of $\theta$ for different $|z|$ with the same values of $\alpha$ and $\lambda$ and truncation index $s = 2$. In this case the coefficients $c_s^{(1,2)}$ can be

[2]We have adopted the convention in the tables of writing $x(y)$ for $x \times 10^y$.

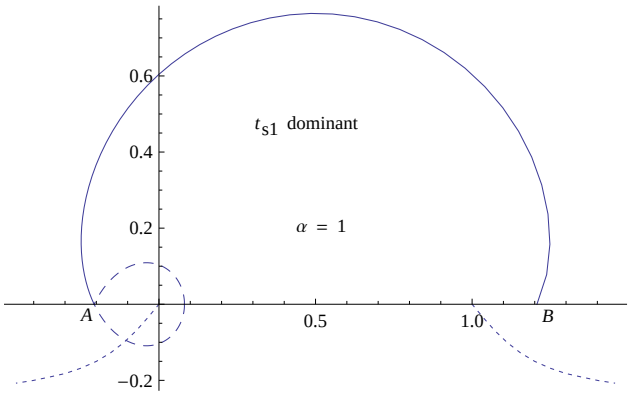


Figure 3: The curve (shown solid) in the $z$-plane on which $\Re\psi(t_{s1}) = \Re\psi(t_{s2})$ when $\alpha = 1$. The endpoints $A$ and $B$ are situated at $z_d^- \doteq -0.2071$ and $z_d^+ \doteq 1.0271$ corresponding to the double saddle points in the $t$-plane. The dashed loop surrounding $z = 0$ shows the curve on which $\Im\psi(t_{s1}) = \Im\psi(t_{s2})$, where a Stokes phenomenon occurs; the interior of this domain is labelled $\mathcal{D}$. The dotted curves issuing from $z = 0$ and $z = 1$ indicate where $t_{s2}$ and $t_{s2} - 1$, respectively, pass onto an adjacent Riemann sheet in the $t$-plane.

obtained alternatively from (2.10). In the column corresponding to $|z| = 0.06$, all the values of $z$ lie in the domain $\mathcal{D}$ in which only the saddle $t_{s1}$ contributes to $F_\alpha(\lambda; z)$. In the column corresponding to $|z| = 0.25$, the error is seen to become relatively large when $\theta = \pi$. This is due to the fact that $z = -0.25$ lies close to the value $z_d^- = -0.2071$, which corresponds to the formation of a double saddle point where the expansion (2.12) ceases to be valid.

Table 1: Values of the absolute relative error in the computation of $F_\alpha(\lambda; z)$ for different truncation index $s$ in the expansions (2.12) and (2.13) when $\lambda = 80$, $\alpha = 1$ and $z = 0.50e^{i\theta}$.

| $s$ | $\theta = 0$ | $\theta = 0.25\pi$ | $\theta = 0.50\pi$ | $\theta = 0.75\pi$ | $\theta = \pi$ |
|---|---|---|---|---|---|
| 0 | 1.042(−08) | 1.865(−03) | 3.251(−03) | 9.873(−04) | 6.525(−04) |
| 1 | 5.158(−07) | 2.927(−06) | 1.619(−05) | 1.219(−05) | 3.182(−05) |
| 2 | 2.731(−08) | 3.390(−08) | 3.139(−07) | 4.098(−07) | 1.617(−06) |
| 3 | 3.050(−11) | 7.929(−10) | 7.240(−09) | 1.910(−08) | 1.213(−07) |
| 4 | 2.166(−12) | 9.013(−12) | 2.263(−10) | 1.175(−09) | 1.195(−08) |
| 5 | 1.473(−15) | 2.314(−13) | 8.728(−12) | 8.961(−11) | 1.464(−09) |

Table 2: Values of the absolute relative error in the computation of $F_\alpha(\lambda; z)$ for different $\theta$ and $|z|$ in the expansions (2.12) and (2.13) when $\lambda = 80$, $\alpha = 1$ and truncation index $s = 2$.

| $\theta/\pi$ | $\lvert z\rvert = 0.06$ | $\lvert z\rvert = 0.25$ | $\lvert z\rvert = 0.50$ | $\lvert z\rvert = 0.75$ | $\lvert z\rvert = 1.00$ | $\lvert z\rvert = 1.20$ |
|---|---|---|---|---|---|---|
| 0 | 1.340(−08) | 3.566(−08) | 2.731(−08) | 3.566(−08) | — | — |
| 0.25 | 4.546(−08) | 7.760(−08) | 3.390(−08) | 4.584(−08) | 9.869(−08) | 1.265(−08) |
| 0.50 | 2.064(−07) | 5.200(−07) | 3.139(−07) | 2.347(−08) | 1.150(−08) | 7.116(−09) |
| 0.75 | 8.228(−07) | 1.159(−05) | 4.098(−07) | 9.420(−08) | 3.681(−08) | 2.153(−08) |
| 1.00 | 1.522(−06) | 7.823(−03) | 1.617(−06) | 1.860(−07) | 5.337(−08) | 2.547(−08) |
| −0.25 | 4.848(−08) | 4.754(−08) | 1.300(−08) | 4.925(−09) | 1.171(−08) | 1.265(−08) |
| −0.50 | 1.597(−07) | 2.028(−07) | 5.965(−08) | 2.347(−08) | 1.150(−08) | 7.116(−09) |
| −0.75 | 6.302(−07) | 3.990(−06) | 4.098(−07) | 9.420(−08) | 4.681(−08) | 2.153(−08) |

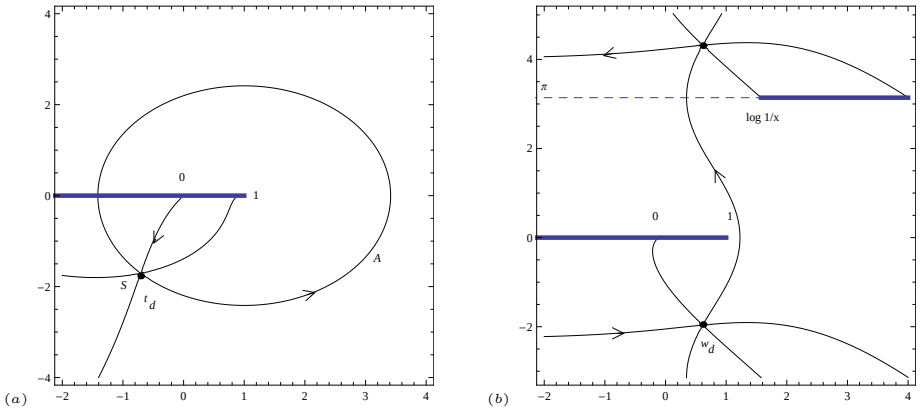


Figure 4: An example of the steepest descent and ascent paths when $z=\frac{1}{2}(1-\sqrt{1+\alpha^2})$ and $\alpha=1$. (a) In the $t$-plane with the double saddle at $t_d$. The steepest descent path $SA$ passes over onto the adjacent Riemann sheet and spirals into the origin. (b) The same situation viewed in the $w$-plane where $w_d=\log t_d$. The saddles are denoted by heavy dots and the arrows indicate the integration path. There is a branch cut along $(-\infty,1]$ and from the point $1/z$ out to infinity (not shown in (a)).

**2.3 The expansion in the general case** The hypergeometric function in (1.1) has the integral representation from (2.3) given by

$$F\left(\begin{array}{c}a-\lambda,b+\lambda\\ c+i\alpha\lambda\end{array};z\right)=\frac{\Gamma(c+i\alpha\lambda)\Gamma(1+b-c+\lambda\beta)}{2\pi i\,\Gamma(b+\lambda)}\int_0^{(1+)}f(t)e^{\lambda\psi(t)}dt,$$

where the amplitude function $f(t)$ is now given by

$$f(t)=\frac{t^{b-1}(t-1)^{c-b-1}}{(1-zt)^a}\ . \tag{2.14}$$

The phase function $\psi(t)$ is as in (2.5) and consequently the distribution of the saddle points remains the same. It therefore follows that the expansion of $F(a-\lambda,b+\lambda;c+i\alpha\lambda;z)$ for $\lambda\to+\infty$ is given by (2.12) and (2.13) with $f(t)$ replaced by (2.14) and the coefficients $c_s^{(1,2)}$ determined from either (2.10) or (2.11). The function $G_\alpha(\lambda)$ is replaced by $\Gamma(c+i\alpha\lambda)\Gamma(1+b-c+\lambda\beta)/\Gamma(b+\lambda)$.

## 3. The expansion when $z=z_d^-$ for $\lambda\to+\infty$

When $z=z_d^-=\frac{1}{2}(1-\sqrt{1+\alpha^2})$, it is seen from (2.7) that the saddles $t_{s1}$ and $t_{s2}$ coalesce to form a double saddle at the point

$$t_d=\frac{z_d^-+\frac{1}{2}i\alpha}{(1+i\alpha)z_d^-}=\frac{1-\sqrt{1+\alpha^2}+i\alpha}{(1+i\alpha)(1-\sqrt{1+\alpha^2})}. \tag{3.1}$$

In the neighbourhood of the point $z=z_d^-$ the expansions in (2.12) and (2.13) break down. In this section we determine the expansion of $F_\alpha(\lambda;z)$ and also that of the general case in (1.1) valid at the coalescence point $z=z_d^-$. The integration path when $z=z_d^-$ is typically as shown in Fig. 4.

**3.1 The expansion of $F_\alpha(\lambda;z_d^-)$.** If we put

$$-u=\psi(t)-\psi(t_d)=A\tau^3+B\tau^4+C\tau^5+D\tau^6+\ldots,\qquad \tau:=t-t_d$$

we find the coefficients

$$A=\frac{-(1+i\alpha)^3}{6\alpha^2\sqrt{1+\alpha^2}}\left\{\alpha^2(-3+\sqrt{1+\alpha^2})+4(-1+\sqrt{1+\alpha^2})\right\},$$

$$B=\frac{(1+i\alpha)^3(\alpha+2i)}{8\alpha^3(1-i\alpha)}\Big\{\alpha^4-4\alpha^2(-2+\sqrt{1+\alpha^2})-8(-1+\sqrt{1+\alpha^2})\Big\},$$

$$C=\frac{(1+i\alpha)^4(6-5i\alpha-\alpha^2)}{20\alpha^4(1-i\alpha)\sqrt{1+\alpha^2}}\Big\{\alpha^4(-5+\sqrt{1+\alpha^2})+4\alpha^2(-5+3\sqrt{1+\alpha^2})+16(-1+\sqrt{1+\alpha^2})\Big\},$$

$$D=\frac{-i(1+i\alpha)^4}{24\alpha^5(1-i\alpha)^2}(8-9i\alpha-3\alpha^2)\Big\{\alpha^6-6\alpha^4(-3+\sqrt{1+\alpha^2})-16\alpha^2(-3+2\sqrt{1+\alpha^2})$$
$$-32(-1+\sqrt{1+\alpha^2})\Big\},\ldots\ .$$

Inversion yields

$$\tau(w)=\frac{w^{1/3}}{A^{1/3}}-\frac{Bw^{2/3}}{9A^{5/3}}+\frac{(B^2-AC)w}{3A^3}-\frac{w^{4/3}}{81A^{13/3}}\,(35B^3-63ABC+27A^2D)+O(w^{5/3}),\quad(3.2)$$

where $w=ue^{\pi i}$ on the path $OS$ and $w=ue^{-\pi i}$ on the path $SA$ in Fig. 4(a). In addition, with

$$T:=t_d-1=\frac{i\alpha\sqrt{1+\alpha^2}}{(1+i\alpha)(1-\sqrt{1+\alpha^2})},\qquad(3.3)$$

we have

$$f(t)=\frac{1}{(t-1)}=\frac{1}{T}\left(1+\frac{\tau}{T}\right)^{-1}=\frac{1}{T}\Big\{1-\frac{w^{1/3}}{A^{1/3}T}+\frac{w^{2/3}}{A^{2/3}T^2}\left(1+\frac{BT}{3A}\right)$$
$$-\frac{w}{AT^3}\left(1+\frac{B^2T^2}{3A^2}+\frac{T}{3A}(2B-CT)\right)+O(w^{4/3})\Big\}.$$

Upon differentiation of $\tau(w)$, we then obtain the expansion

$$\frac{1}{t-1}\,\frac{d\tau}{dw}=\sum_{m=0}^{\infty}\mathcal{B}_m(\alpha)w^{(m-2)/3}\qquad(3.4)$$

valid in a neighbourhood of $w=0$ ($t=t_d$), where

$$\mathcal{B}_0(\alpha)=\frac{1}{3A^{1/3}T},\quad \mathcal{B}_1(\alpha)=-\frac{1}{9A^{2/3}T^2}\left(3+\frac{2BT}{A}\right),$$

$$\mathcal{B}_2(\alpha)=\frac{1}{3AT^3}\left\{1+\frac{BT}{A}\left(1+\frac{BT}{A}\right)-\frac{CT^2}{A}\right\},$$

$$\mathcal{B}_3(\alpha)=-\frac{1}{243A^{4/3}T^4}\left\{81+140\frac{B^3T^3}{A^3}+\frac{126BT^2}{A^2}(B-2CT)+\frac{108T}{A}(B-CT+DT^2)\right\},\ldots\ .\quad(3.5)$$

The coefficients $A$, $B$, $C$, $D$ and the quantity $T$ are defined above in terms of the parameter $\alpha$.

Then, from (2.4) and (3.4), we obtain

$$\begin{aligned}F_\alpha(\lambda;z_d^-)&=\frac{G_\alpha(\lambda)e^{\lambda\psi(t_d)}}{2\pi i}\int_0^\infty e^{-\lambda u}\left\{\frac{1}{t-1}\,\frac{dt}{du}\Big|_{ue^{-\pi i}}-\frac{1}{t-1}\,\frac{dt}{du}\Big|_{ue^{\pi i}}\right\}du\\&\sim-\frac{G_\alpha(\lambda)}{\pi}\,e^{\lambda\psi(t_d)}\int_0^\infty e^{-\lambda u}\sum_{m=0}^{\infty}\mathcal{B}_m(\alpha)u^{(m-2)/3}\sin\pi(\tfrac{1}{3}m+\tfrac{1}{3})\,du\end{aligned}$$

for $\lambda\to+\infty$. This therefore produces the expansion

$$F_\alpha(\lambda;z_d^-)\sim-\frac{G_\alpha(\lambda)}{\pi}\,e^{\lambda\psi(t_d)}\sum_{m=0}^{\infty}\frac{\mathcal{B}_m(\alpha)\Gamma(\frac{1}{3}m+\frac{1}{3})}{\lambda^{(m+1)/3}}\,\sin\pi(\tfrac{1}{3}m+\tfrac{1}{3})\qquad(\lambda\to+\infty).\qquad(3.6)$$

Since $z_d^-$ is real it immediately follows from (2.1) that

$$F_{-\alpha}(\lambda;z_d^-)=\overline{F}_\alpha(\lambda;z_d^-).\qquad(3.7)$$

Due to the complexity of the coefficients it is not practical to present their explicit dependence on the parameter $\alpha$ for more than the first three terms in the expansion (3.6). If, however, $\alpha$ is given a numerical value then the inversion process can be carried out with *Mathematica* to many more terms. In the particular case $\alpha = 1$, the values of the coefficients $\mathcal{B}_m(\alpha)$ are tabulated in Table 3 for $m \leq 10$; we observe that the values of $\mathcal{B}_2(\alpha)$, $\mathcal{B}_5(\alpha)$, $\mathcal{B}_8(\alpha), \ldots$ are not required. Values of $F_\alpha(\lambda; z_d^-)$ and its asymptotic estimate from (3.6) with $m \leq 10$ (sub-optimal truncation) are given in Table 4.

Table 3: Values of the coefficients $\mathcal{B}_m(\alpha)$ to 10dp for $m \leq 10$ when $\alpha = 1$.

| $m$ | $\mathcal{B}_m(\alpha)$ | $m$ | $\mathcal{B}_m(\alpha)$ |
|---|---|---|---|
| 0 | $+1.1210852199 + 0.3003938793i$ | 6 | $+0.0251806251 + 0.0067471281i$ |
| 1 | $+0.2166214717 + 0.8084423383i$ | 7 | $-0.0018434584 - 0.0068798804i$ |
| 3 | $+0.0700678262 + 0.0187746174i$ | 9 | $+0.0044976298 + 0.0012051363i$ |
| 4 | $+0.0082200112 + 0.0306774994i$ | 10 | $-0.0001979294 - 0.0007386825i$ |

Table 4: Values of $F_\alpha(\lambda; z_d^-)$ and the asymptotic approximation (3.6) with $m \leq 10$ when $\alpha = 1$.

| $\lambda$ | $F_\alpha(\lambda; z_d^-)$ | Asymptotic value |
|---|---|---|
| 10 | $-1.360471986485 - 1.001859460942i$ | $-1.360471\mathbf{9}37691 - 1.00185\mathbf{9}4\mathbf{3}5166i$ |
| 20 | $+0.594081476620 + 1.768757533401i$ | $+0.59408147\mathbf{5}031 + 1.76875753\mathbf{0}253i$ |
| 40 | $-1.652642124543 + 1.239971720906i$ | $-1.65264212\mathbf{4}37\mathbf{3} + 1.23997172\mathbf{0}74\mathbf{2}i$ |
| 60 | $-1.790341054904 - 1.271041237802i$ | $-1.79034105\mathbf{4}8\mathbf{6}1 - 1.27104123\mathbf{7}7\mathbf{8}i$ |
| 80 | $+0.702398854959 - 2.183378031108i$ | $+0.70239885495\mathbf{5} - 2.18337803109\mathbf{2}i$ |
| 100 | $+2.373096383290 + 0.016497731931i$ | $+2.37309638328\mathbf{4} + 0.01649773193\mathbf{2}i$ |

A uniform approximation for $F_\alpha(\lambda; z)$ for $z \simeq z_d^-$ could be obtained by making the standard cubic transformation (see [11, (2.4.18)]) to $\psi(t)$ in (2.4). We do not pursue this further here.

**3.2 The expansion in the general case when $z = z_d^-$.** The expansion of the hypergeometric function in (1.1) for general $a$, $b$ and $c$ when $z = z_d^-$ follows a similar procedure to that in the specific case of $F_\alpha(\lambda; z)$. The amplitude function $f(t)$ is now given by (2.14), which may be expressed in the neighbourhood of the double saddle $t_d$ as (with $t = t_d + \tau$)

$$f(t) = \frac{t^{b-1}(t-1)^{c-b-1}}{(1 - z_d^- t)^a} = \frac{1}{\hat{T}}\,(1 + \frac{\tau}{T})^{c-b-1} \frac{(1 + \frac{\tau}{t_d})^{b-1}}{(1 - \frac{\kappa\tau}{t_d})^a},$$

where $T$ is defined in (3.3) and

$$\kappa := \frac{z_d^- t_d}{1 - z_d^- t_d} = \frac{1 - \sqrt{1+\alpha^2} + i\alpha}{1 + \sqrt{1+\alpha^2} + i\alpha}, \qquad \hat{T}^{-1} := \frac{t_d^{b-1}(t_d - 1)^{c-b-1}}{(1 - z_d^- t_d)^a}\ .$$

Expansion about $\tau = 0$, followed by use of (3.2) to express $\tau$ in terms of $w$, produces

$$\log\, f(t) = -\log \hat{T} + \sum_{n=1}^{\infty} \gamma_n \left(\frac{w}{A}\right)^{n/3},$$

where

$$\gamma_1 = \frac{c-b-1}{T} + \frac{b-1+\kappa a}{t_d}, \qquad \gamma_2 = -\frac{b-1-\kappa^2 a}{2t_d^2} - \frac{c-b-1}{2T^2} - \frac{\gamma_1 B}{3A},$$
$$\gamma_3 = \frac{(B^2 - 3AC)\gamma_1}{9A^2} - \frac{2B\gamma_2}{3A} + \frac{b-1+\kappa^3 a}{3t_d^3} + \frac{c-b-1}{3T^3}, \ldots .$$

Application of Lemma 1 in the appendix therefore shows that

$$f(t)=\frac{1}{\hat{T}}\biggl\{1+\sum_{n=0}^{\infty}D_n\biggl(\frac{w}{A}\biggr)^{n/3}\biggr\},$$

where

$$D_1=\gamma_1,\quad D_2=\tfrac{1}{2}\gamma_1^2+\gamma_2,\quad D_3=\tfrac{1}{6}\gamma_1^3+\gamma_1\gamma_2+\gamma_3,\ldots\,.$$

Then, from (3.2) we obtain the result

$$f(t)\frac{dt}{dw}=\sum_{m=0}^{\infty}\hat{B}_m(\alpha)w^{(m-2)/3}$$

valid near $w=0$ ($t=t_d$), where the first three contributory coefficients are[3]

$$\hat{B}_0(\alpha)=\frac{1}{3A^{1/3}\hat{T}},\qquad \hat{B}_1(\alpha)=\frac{1}{9A^{2/3}\hat{T}}\biggl\{3\biggl(\frac{c-b-1}{T}+\frac{b-1+\kappa a}{t_d}\biggr)-\frac{2B}{A}\biggr\},$$

$$\hat{B}_3(\alpha)=-\frac{1}{243A^{4/3}\hat{T}}\biggl\{\frac{4}{A^3}(35B^3-63ABC+27A^2D)-\frac{81}{A^2}(B^2-AC)D_1+\frac{54BD_2}{A}-81D_3\biggr\}. \quad (3.8)$$

From this we find the expansion

$$F\left(\begin{array}{c}a-\lambda,b+\lambda\\ c+i\alpha\lambda\end{array};z\right)\sim\frac{\Gamma(c+i\alpha\lambda)\Gamma(1+b-c+\lambda\beta)}{\Gamma(b+\lambda)}\,\frac{e^{\lambda\psi(t_d)}}{\pi}$$

$$\times\sum_{m=0}^{\infty}\hat{B}_m(\alpha)\frac{\Gamma(\frac{1}{3}m+\frac{1}{3})}{\lambda^{(m+1)/3}}\,\sin\pi(\tfrac{1}{3}m+\tfrac{1}{3})\qquad(\lambda\to+\infty). \quad (3.9)$$

The complexity of the higher contributory coefficients $\hat{B}_m(\alpha)$ ($m\geq 4$) is such that there appears to be little value in their presentation, although in specific cases with numerical values for $a$, $b$, $c$ and $\alpha$ it would be quite feasible to continue the inversion process to higher order. It can be verified with some effort that when $a=0$, $b=c=1$ we have $\hat{T}=T$ and the coefficients in (3.8) reduce to those given in (3.5).

## 4. Application to the expansion of the Legendre functions

From (1.3) and (1.4) we have the Legendre functions of degree $\lambda$ and order $-i\alpha\lambda$, where $\alpha>0$, $\lambda>0$, given by

$$P_{\lambda}^{-i\alpha\lambda}(x)=\frac{1}{\Gamma(1+i\alpha\lambda)}\left(\frac{x-1}{x+1}\right)^{i\alpha\lambda/2}F_{\alpha}(\lambda;\tfrac{1}{2}-\tfrac{1}{2}x), \quad (4.1)$$

$$e^{-\pi\alpha\lambda}Q_{\lambda}^{-i\alpha\lambda}(x)=\frac{\Gamma(-i\alpha\lambda)}{2}\left(\frac{x-1}{x+1}\right)^{i\alpha\lambda/2}F_{\alpha}(\lambda;\tfrac{1}{2}-\tfrac{1}{2}x)$$

$$+\frac{\Gamma(i\alpha\lambda)\Gamma(1+\lambda\beta)}{2\Gamma(1+\lambda\overline{\beta})}\left(\frac{x-1}{x+1}\right)^{-i\alpha\lambda/2}F_{-\alpha}(\lambda;\tfrac{1}{2}-\tfrac{1}{2}x), \quad (4.2)$$

where $F_{\alpha}(\lambda;z)$ is defined in (1.2) and $F_{-\alpha}(\lambda;\frac{1}{2}-\frac{1}{2}x)$ is given by the conjugate relation (2.1). These functions are defined[4] in the complex $x$-plane cut along $(-\infty,1]$. The expansions for $P_{\lambda}^{\pm i\alpha\lambda}(x)$ and $Q_{\lambda}^{\pm i\alpha\lambda}(x)$ then follow from that of $F_{\alpha}(\lambda;z)$ given in (2.12) and (2.13).

In the special case $x=\sqrt{1+\alpha^2}$, the argument of $F_{\pm\alpha}(\lambda;\frac{1}{2}-\frac{1}{2}x)$ is equal to

$$z_d^{-}=\tfrac{1}{2}(1-\sqrt{1+\alpha^2})$$

[3]We omit the coefficient $\hat{B}_2(\alpha)$ as this is not required.

[4]In *Mathematica* they are obtained numerically by use of the 'type-3' Legendre functions.

in (2.8). This corresponds to the coincidence of the two saddle points associated with the integral for $F_\alpha(\lambda;z)$. From the expansion in (3.6), it therefore follows that

$$P_\lambda^{-i\alpha\lambda}(\sqrt{1+\alpha^2}) \sim -\frac{\Gamma(1+\lambda\beta)}{\Gamma(1+\lambda)}\left(\frac{\sqrt{1+\alpha^2}-1}{\sqrt{1+\alpha^2}+1}\right)^{i\alpha\lambda/2}\frac{e^{\lambda\psi(t_d)}}{\pi}\,S(\lambda;\alpha) \tag{4.3}$$

and

$$Q_\lambda^{-i\alpha\lambda}(\sqrt{1+\alpha^2}) \sim \frac{e^{\pi\alpha\lambda}}{\sinh\pi\alpha\lambda}\,\frac{\Gamma(1+\lambda\beta)}{\Gamma(1+\lambda)}\,\Im\left\{\left(\frac{\sqrt{1+\alpha^2}-1}{\sqrt{1+\alpha^2}+1}\right)^{i\alpha\lambda/2} e^{\lambda\psi(t_d)}\,S(\lambda;\alpha)\right\} \tag{4.4}$$

as $\lambda\to+\infty$, where

$$S(\lambda;\alpha) := \sum_{m=0}^\infty \frac{\mathcal{B}_m(\alpha)\Gamma(\frac{1}{3}m+\frac{1}{3})}{\lambda^{(m+1)/3}}\,\sin\pi(\tfrac{1}{3}m+\tfrac{1}{3}),$$

$t_d$ is given in (3.1) and $\psi(t)$ is defined in (2.5).

The expansions for the functions with positive imaginary order then follow from

$$P_\lambda^{i\alpha\lambda}(\sqrt{1+\alpha^2}) = \overline{P}_\lambda^{\,-i\alpha\lambda}(\sqrt{1+\alpha^2})$$

and [11, (14.9.14), (14.3.10)]

$$Q_\lambda^{i\alpha\lambda}(\sqrt{1+\alpha^2}) = \frac{\Gamma(1+\lambda\overline{\beta})}{\Gamma(1+\lambda\beta)}\,e^{-2\pi\alpha\lambda}\,Q_\lambda^{-i\alpha\lambda}(\sqrt{1+\alpha^2}).$$

## Appendix: The expansion of $G_\alpha(\lambda)$

In this appendix we consider the expansion of $G_\alpha(\lambda)$ in (2.6) in inverse powers of $\lambda$. This is given for completeness as the main asymptotic problem under consideration is the large-$\lambda$ expansion of the integral appearing in (2.4).

It is sufficient to consider $\alpha>0$ since the value of $G_\alpha(\lambda)$ for $\alpha<0$ is given by its conjugate (when $\lambda>0$). We use the well-known expansion for $\log\Gamma(z)$ as $|z|\to\infty$ is [11, p. 141]

$$\log\Gamma(z) \sim (z-\frac{1}{2})\log z - z + \frac{1}{2}\log 2\pi + \sum_{k=1}^\infty \frac{B_{2k}}{2k(2k-1)z^{2k-1}} \qquad (|\arg z|<\pi),$$

where $B_{2k}$ denote the even-order Bernoulli numbers. In addition, we have the following lemma [2]:

**Lemma 1**. *Let $S(x)=\sum_{n=1}^\infty a_n x^{-n}$ as $x\to\infty$ be a given expansion. Then the composition* $\exp[S(x)]$ *has the asymptotic expansion of the following form*[5]

$$\exp[S(x)] \sim \sum_{n=0}^\infty b_n x^{-n} \qquad (x\to\infty)$$

*where*

$$b_0=1, \qquad b_n = \frac{1}{n}\sum_{k=1}^n k a_k b_{n-k} \qquad (n\geq 1).$$

Then it follows that

$$\log\left(\frac{G_\alpha(\lambda)}{i\alpha\beta\lambda}\right) = \log\frac{\Gamma(i\alpha\lambda)\Gamma(\lambda\beta)}{G_\alpha(\lambda)}$$

$$\sim \frac{1}{2}\log\frac{2\pi}{\lambda} + (i\alpha\lambda-\frac{1}{2})\log\imath\alpha + (\lambda\beta-\frac{1}{2})\log(1-i\alpha) + \sum_{k=1}^\infty \frac{A_k}{\lambda^{2k-1}}$$

[5]The coefficients $b_n$ can also be expressed in terms of the complete Bell polynomial $B_n$ in the form $b_n = B_n(1!a_1, 2!a_2, \ldots, n!a_n)/n!$.

as $\lambda \to +\infty$, where

$$A_k := \frac{B_{2k}}{2k(2k-1)}\left\{\frac{1}{(i\alpha)^{2k-1}} + \frac{1}{(1-i\alpha)^{2k-1}} - 1\right\}.$$

Some straightforward algebra and application of Lemma 1 then produces

$$\begin{aligned} G_\alpha(\lambda) &\sim \sqrt{2\pi\lambda\alpha}\,(1+\alpha^2)^{\frac{1}{2}\lambda+\frac{1}{4}} e^{-\lambda\alpha(\frac{1}{2}\pi+\phi)+i\Phi} \exp\left\{\sum_{k=1}^{\infty} \frac{A_k}{\lambda^{2k-1}}\right\} \\ &\sim \sqrt{2\pi\lambda\alpha}\,(1+\alpha^2)^{\frac{1}{2}\lambda+\frac{1}{4}} e^{-\lambda\alpha(\frac{1}{2}\pi+\phi)+i\Phi} \left\{1 + \sum_{k=1}^{\infty} \frac{E_k}{\lambda^k}\right\} \qquad (\lambda \to +\infty) \end{aligned} \tag{A.1}$$

where

$$\Phi := \lambda\alpha \log\left(\frac{\alpha}{\sqrt{1+\alpha^2}}\right) - (\lambda + \tfrac{1}{2})\phi + \tfrac{1}{4}\pi$$

with $\phi$ defined in (2.2). The first few coefficients $E_k$ are

$$E_1 = A_1, \quad E_2 = \tfrac{1}{2}A_1^2, \quad E_3 = \tfrac{1}{6}A_1^3 + A_2, \quad E_4 = \tfrac{1}{24}A_1^4 + A_1A_2,$$

$$E_5 = \tfrac{1}{120}A_1^5 + \tfrac{1}{2}A_1^2A_2 + A_3, \quad E_6 = \tfrac{1}{720}A_1^6 + \tfrac{1}{6}A_1^3A_2 + \tfrac{1}{2}A_2^2 + A_1A_3, \ldots .$$

# References


[1] N. Bleistein and R.A. Handelsman, Asymptotic Expansions of Integrals, Dover, New York 1986.

[2] C.-P. Chen, N. Elezović and L. Vukšić, Asymptotic formulae associated with the Wallis power function and digamma function, J. Classical Anal. **2** (2013) 151–166.

[3] T.M. Cherry, Asymptotic expansions for the hypergeometric functions occurring in gas-flow theory, Proc. Roy. Soc. London **A202** (1950) 507–522.

[4] M. Cvitković, A.-S. Smith and J. Pande, General asymptotic expansions of the hypergeometric function with two large parameters. arXiv:1602.05146 (2016).

[5] R.B. Dingle, *Asymptotic Expansions: Their Derivation and Interpretation*, Academic Press, London 1973.

[6] T.M. Dunster, Uniform asymptotic solutions of second-order linear differential equations having a double pole with complex exponent and a coalescing turning point, SIAM J. Math. Anal. **21** (1990) 1594–1618.

[7] D.S. Jones, Asymptotics of the hypergeometric function, Math. Meth. Appl. Sci. **24** (2001) 369–389.

[8] M.J. Lighthill, The hodograph transformation in trans-sonic flow. II Auxiliary theorems on the hypergeometric functions $\psi_n(\tau)$. Proc. Roy. Soc. London **A191** (1947) 341–351.

[9] A.B. Olde Daalhuis, Uniform asymptotic expansions for hypergeometric functions. I, II. Anal. Appl. (Singap.) **1** (2003) 111–120, 121–128.

[10] F.W.J. Olver, *Asymptotics and Special Functions*, Academic Press, New York 1974. Reprinted A.K. Peters, Massachussets 1997.

[11] F.W.J. Olver, D.W. Lozier, R.F. Boisvert and C.W. Clark (eds.), *NIST Handbook of Mathematical Functions*, Cambridge University Press, Cambridge 2010.

[12] R.B. Paris, *Hadamard Expansions and Hyperasymptotic Evaluation: An Extension of the Method of Steepest Descents*, Cambridge University Press, Cambridge 2011.

[13] R.B. Paris Asymptotics of the Gauss hypergeometric function with large parameters, I., J. Classical Anal. **2** (2013) 183–203.

[14] R.B. Paris Asymptotics of the Gauss hypergeometric function with large parameters, II., J. Classical Anal. **3** (2013) 1–15.

[15] N.M. Temme, *Asymptotic Methods for Integrals*, Series in Analysis vol. 6, World Scientific, New Jersey 2015.

[16] G.N. Watson, Asymptotic expansions of hypergeometric functions, Trans. Cambridge Philos. Soc. **22** (1918) 277–308.

[17] A. Vainchtein, Y. Starosvetsky, J.D. Wright and R. Perline, Solitary waves in diatomic chains, Phys. Rev. E**93** (2016) 042210.

[18] J. Wojdylo, On the coefficients that arise from Laplace's method, J. Comput. Appl. Math. **196** (2006) 241–266.

[19] J.D. Wright, Private communication (2015).